

Investigation on the binding affinity of five drug-like sulphonamides on SARS-CoV-2 targets: A computational study

Bindu T K, Vinod P Raphael* & Shaju K S

Department of Chemistry, Government Engineering College, Thrissur 680 009, Kerala, India

E-mail: vinodraphael@gectcr.ac.in, bindutk@gectcr.ac.in, shajuks@gectcr.ac.in

Received 1 August 2023; accepted (revised) 21 December 2023

Covid-19 is a dreadful pandemic of the 21st century. Many people have lost their lives and those who recovered are ailing from serious health issues. Even though preventive vaccinations are being carried out all over the world, lack of effective drugs to cure the patients increases the casualties. Scientists are in search of effective pharmaceuticals to fight against coronavirus. Computational methods are used for the discovery of new drugs. In the present course of investigation, we have performed docking studies of fifteen molecules on various targets of SARS-CoV-2, and five drug like molecules having high binding scores have been selected and reported. The molecules under investigation have been selected from spirochem and ChemBL databases. They are the derivatives of benzene sulphonamide and consist of cubane or cyclopropane or cyclobutane ring systems. Web Servers like Swissdock and SwissADME have been used for docking studies and ADME prediction respectively. Softwares such as Chimera and Biovia Discovery Studio have been employed for the modeling of the protein ligand-complex. Structures of drug targets of coronavirus have been downloaded from Protein Data Bank. Ligands w045 and 2059020 have been effective against the main protease of SARS-CoV-2. The nucleoprotein of the virus is well inhibited by 205913 and 2059020. The envelope protein of the virus shows great attraction towards the molecule 2059020. The same ligand also shows better binding capacity on the surface of the spike protein of the covid-19 virus.

Keywords: SARS-CoV-2, Docking, Sulphonamide, SwissADME

SARS-CoV-2 has become one of the most spreading and destructive pathogens which lead to the pandemic Covid-19. The emergence of this pathogen was first noted in Wuhan, China towards the end of 2019. Within a few months it spread all over the world. Affected patients may have symptoms like nasal congestion, fever, dry cough, sore throat, *etc.* in the early stage and eventually they may develop shortness of breath, diarrhea, and pneumonia^{1,2}.

To minimize the spread of covid-19, the World Health Organization (WHO) announced a public health emergency and many countries around the world declared complete lockdown for weeks. As of 1st August 2023, 69 lakh people lost their lives due to this pandemic³. Laborious investigations are being conducted by biotechnologists and microbiologists to find out effective vaccines for covid-19. As a result of this rigorous work some effective vaccines were discovered by the scientists and are being given to the people. Covishield (Name in India for AstraZeneca vaccine of Oxford, U. K), Covaxin, Sputnik V, Pfizer are the commercial names of some effective vaccines⁴⁻¹¹. Though the vaccination drive is going on throughout the world, the rate of spread of the

pandemic is higher than the rate of vaccination, especially in countries like India. To reduce the rate of mortality effective antiviral drugs have to be discovered. The treatment of covid-19 patients will be tedious in severe cases due to the lack of effective drugs. Pharmaceutical chemists and medical practitioners are involved in rigorous research to invent the suitable drugs to fight coronavirus. Some studies showed that the anti-viral Remdesivir has a moderate percentage of efficacy in treating covid-19¹²⁻¹⁴. Some doctors suggest the combination of anti-HIV agents Favipiravir- Lopinavir for the treatment of covid-19¹⁵⁻¹⁷.

For the development of a therapeutic drug having great efficacy, knowledge of the drug targets is important. The SARS-CoV-2 virus is an RNA virus that consists of various structural protein molecules¹⁸. The main RNA of a virus is associated with nucleocapsid protein which plays an important role in the multiplication of the virus. The nucleus of coronavirus is encapsulated with envelope proteins and membrane proteins. It is the spike glycoproteins protruding from the surface membrane which is instrumental in binding with the human cells¹⁹⁻²².

During replication and translation of the virus, certain enzymes and proteins are involved. These are called non-structural proteins. The possibility of inhibiting the non-structural proteins to prevent replication and translation is also important in the drug discovery process. The following paragraphs depict the details of possible drug targets of covid-19.

Drug targets of SARS-CoV-2

Structural Proteins

Nucleocapsid protein (NP)

The principal role of the N-arm of nucleocapsid protein is the viral RNA binding^{23,24}. The C-terminal part of N proteins helps the replication and transcription process of viral RNA. Molecules that make a strong complex with the C-terminal/N-terminal segments of nucleocapsid protein may prevent the multiplication of viral particles.

Envelope protein (EP)

Envelope protein comprises a hydrophobic part and charged cytoplasmic end^{25,26}. This is the smallest structural protein of SARS-CoV-2. Envelope proteins take part in the development of the shape of a cell (morphogenesis). Ion channels are created due to the oligomerization of E proteins. This structural protein also helps the assembly and envelope formation of corona viral particles. Research data shows that coronavirus without E protein may act as potential vaccine candidates. Thus E protein can be selected as a suitable drug target for inhibiting the growth of SARS-CoV-2²⁷. The agglomeration of five amino acid chains having 31 segments leads to the complete structure of E protein. The inner core of the envelope protein is largely hydrophobic than the outer surface.

Spike glycoprotein (SP)

Spike glycoprotein present on the surface of the covid-19 virus plays an important role in the invasion of the virus into the receptor cell (ACE2 present in the lungs)^{28,29}. The closed structure of spike protein (PDB id: 6VXX) consists of three chains. Chain A of the spike protein consists of S1 and S2 subunits. The S1 subunit is mainly responsible for the invasion of the coronavirus to the host cells. Chain A acts as the receptor binding chain and the upper lobe of the chain can be termed as Receptor Binding Domain (RBD). The key step in the binding process of coronavirus to the ACE2 epithelial cells is the interaction of the RBD with ACE2 protein^{30,31}. The receptor-binding domain of the spike glycoprotein is thus considered as the target for antibodies and drugs³². The six amino acids

present in the RBD (Leu455, Phe486, Gln493, Ser494, Asn501, and Tyr505) of spike glycoprotein of SARS-CoV-2 mainly involve in the binding process with ACE2.

Non-structural proteins (NSP)

These are proteins cleaved from the polypeptide chain synthesized by the Open Reading frame gene 1ab of SARS-CoV-2. Structures of sixteen non-structural proteins and their functions in the multiplication processes of coronavirus are available from the literature. In the present paper, we took the nonstructural proteins NSP5 and NSP10 as the drug targets³³⁻³⁷. Out of the sixteen proteins, two act as enzymes called proteases (NSP3 and NSP5). The key enzyme of a covid-19 virus is the Main protease (NSP5 or M^{pro}) which has a central role in the multiplication of the virus. NSP5 is a cysteine protease containing a catalytic dyad (His41/Cys145) in its active site. This main protease of SARS-CoV-2 assists the virus in the processes like replication and translation. Since M^{pro} has a significant role in the growth of coronavirus, it can be considered an important drug target.

The NSP10 complex has a significant role in the capping of viral mRNA *via* methylation which helps the efficient translation and to dodge immune surveillance. The capping is initiated by the stimulation of NSP14 and NSP16 by NSP10. Interfering agents for NSP10 like small molecules can prevent the transcription and translation of viral RNA. The skeletal structure of NSP10 protein is a single chain, complexed with zinc ions and consists of 139 amino acids.

In this study, computational evaluation of the molecules obtained from the databases like chemBL and spirochem on various structural and non-structural proteins of SARS-CoV-2 were done. Out of fifteen molecules that possess alicyclic and aromatic moieties in their structures, only five molecules having good binding scores with various target proteins are reported in this article. Structural, pharmacokinetic and the drug likeness of the selected molecules were determined using a web server. The binding affinity of the molecules on the drug target receptors of coronavirus was compared using the docking scores of the protein-ligand complex.

Materials and Methods

The 3D structures of the structural and non-structural protein molecules were downloaded from the RSC protein data bank³⁸. Details like PDB Id,

sequence length, and the technique used for the characterization of protein molecules are listed in Table 1. Fig. 1 shows the skeletal structures of various structural and non-structural proteins of SARS-CoV-2 together with the hydrogen bond surface in the binding site.

Docking studies

After downloading the PDB file of proteins, analysed with Edupymol software³⁹. Co-crystallised ligand molecules and water molecules were removed using Pymol and hydrogen atoms were added. The prepared protein was used for docking studies. The

Table 1 — Details of structural and non- structural proteins of SARS-CoV-2

Protein	PDB Id	Chains	Sequence length	Technique	Ligand
NP	6M3M	A, B, C, D	136	XRD (Resolution 2.70 Å)	Nil
EP	7K3G	A, B, C, D, E	31	Solid State NMR	Nil
NSP5 (M ^{pro})	6LU7	A	306	XRD (Resolution 2.16 Å)	N3
NSP10	6ZCT	A	125	XRD (Resolution 2.55 Å)	Zn ²⁺
SP	6VXX	A(S1 subunit)	1281	Electron Microscopy (Resolution 2.80 Å)	NAG

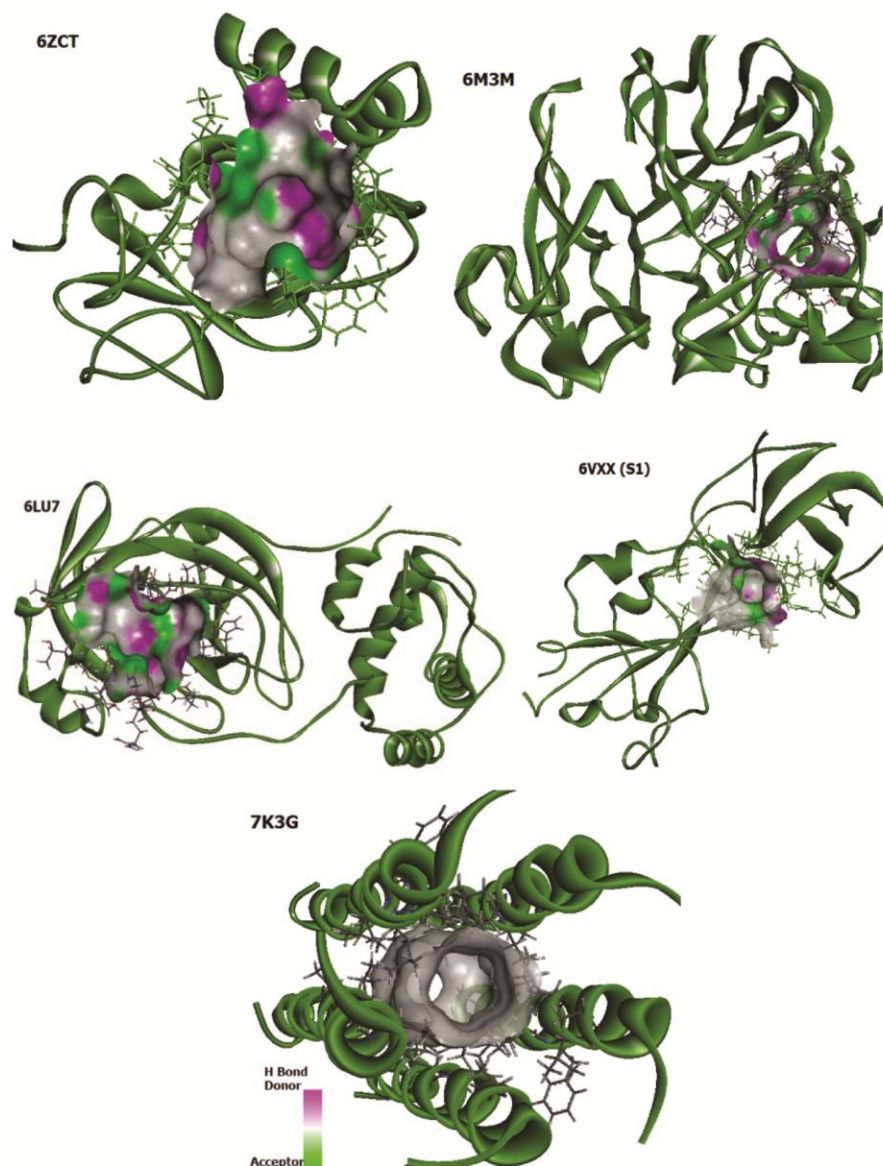


Fig. 1 — 3D structures of various drug targets of SARS-CoV-2 with their binding pocket and hydrogen bond surface

structures of drug-like molecules were downloaded from spirochem⁴⁰ and ChemBL databases⁴¹ and converted into mol2 files using openbabel software. The online web server Swissdock⁴² was used to dock the molecules with the receptor. The results of docking were analyzed using Chimera 1.13rc and Discovery studio 2020⁴³ softwares.

Drug-like molecules

Molecules having an aromatic ring, aliphatic ring, halogens, and sulphonyl groups were considered for the docking purpose. Out of 15 molecules selected from the databases, the molecular structures and docking results of only five are reported in this work. Four molecules were selected from chemBL database (Id: 2059013, 2059019, 2059020, 2059819) and one was taken from spirochem data pool (Id: w045). All the molecules were the derivatives of sulphonamide. The only structural difference between the molecules was in the single substituent present on the tertiary nitrogen atom. One alicyclic ring such as cubane or cyclopropane or cyclobutane was present in every molecule. Molecules with ChemBL numbers 2059019 and 2059020 possessed oxadiazole substituted cyclopropane and cyclobutane ring systems respectively. Molecules with Ids w045, 2059013 and 2059819 consisted of cyanide substituted ring systems. Chemical structures of the molecules and their database numbers are given in Fig. 2.

Results and Discussion

Structural, Pharmacokinetic and Drug Likeness studies

The absorption of a drug is strongly related to the Topological Surface Area (TPSA). It is calculated by adding the surface of polar atoms such as oxygen and nitrogen and the hydrogen atoms attached to these electronegative atoms. If the TPSA value of a molecule is very high, the absorption or the intestinal permeability will be low. To improve the permeability of a molecule the main strategy accepted by a pharmaceutical chemist is to lower the number of hydrogen bond donor sites and hydrogen bonding accepting sites. It is generally accepted that a molecule whose TPSA is less than about 140–150 Å² will have appreciable permeability. From Table 2 it is clear that the TPSA values of the molecules under investigation range between 112.64–127.77 Å²; suggesting that all the molecules have moderate intestinal absorption and permeability. According to SwissADME prediction, the five molecules were moderately soluble in water. This property of the

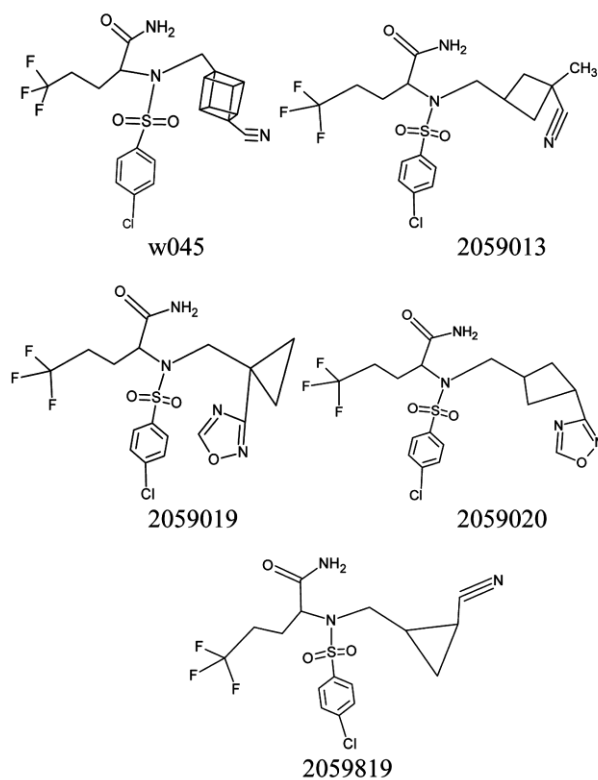


Fig. 2 — Structures of drug like molecules

molecule is also important in determining the drug ability. In general, molecules having very high or low solubilities will not show appreciable drug ability.

LogP of a molecule is an important parameter in predicting the Druglikeness. It gives an idea about the hydrophilic-lipophilic balance of the molecule. If the hydrophilicity of the molecule is too high, it will show low permeability, plasma protein binding capacity, and distribution. SwissADME provides five partition function models and their consensus value. The consensus value of the partition function of the five molecules in the octanol-water system is recorded in Table 2. All the molecules showed appreciable lipophilic nature according to the computational studies. The consensus of LogPo/w of the compounds ranged between 2.67–3.29 and they were suitable for oral administration according to the Lipinski rule. The molecule having chemBL id 2059013 showed highest lipophilicity.

Molar refractivity (MR) is a measure of the polarizability of a molecule. MR is related to the molecular mass, volume, London dispersion forces, and electrostatic potential of the molecule. London dispersion forces are considered as an important component in drug-receptor interaction. Molecules

Table 2 — Physical properties of the molecules predicted by SwissADME

Molecule Id	Mol. wt (g/mol)	TPSA(Å ²)	Consensus of LogP _{o/w}	Water Solubility	Molar Refractivity
W045	485.91	112.64	3.02	Moderately soluble	106.50
2059013	451.89	112.64	3.29	Moderately soluble	100.79
2059019	466.86	127.77	2.84	Moderately soluble	99.11
2059020	480.89	127.77	2.98	Moderately soluble	104.03
2059819	423.84	112.64	2.67	Moderately soluble	91.44

Table 3 — Pharmacokinetics of the molecules predicted by SwissADME

Molecule	GI absorption	BBB permeant	P-gp substrate	CYP1A2 inhibitor	CYP2C19 inhibitor	CYP2C9 inhibitor	CYP2D6 inhibitor	CYP3A4 inhibitor
W045	Low	No	Yes	No	Yes	No	Yes	Yes
2059013	Low	No	No	No	Yes	No	Yes	Yes
2059019	Low	No	No	No	Yes	Yes	No	Yes
2059020	Low	No	Yes	No	Yes	No	Yes	Yes
2059819	High	No	No	No	Yes	No	No	Yes

that are acting as therapeutic agents usually have their MR value in the range 40-130. Molar refractivity of the five molecules considered here fell between 91-107 according to SwissADME.

Drug-drug interactions are an important issue in multi-drug therapies. When drugs are co-administered, one may interact with hepatic cytochrome P450 enzymes which lead to the inhibition or induction by the second drug. The process of inhibition lowers the metabolic process while the induction enhances it. Cytochrome P450 isoenzymes are mainly found in the endoplasmic reticulum of hepatocytes. It has been proved that greater than 90% of the oxidation of drugs are catalyzed by the six CYP enzymes such as CYP1A2, CYP2C19, CYP2C9, CYP2D6, CYP3A4, and CYP2E1. A clear-cut understanding of the pharmacokinetics of enzyme inhibition or induction helps greatly in multi-drug therapies. Identification of individuals who have the risk of giving two drugs simultaneously is possible by these investigations. Table 3 reveals the inhibiting nature of the ligand molecules on various cytochrome enzymes predicted by SwissADME. All the molecules acted as the inhibitor on the enzymes CYP2C19 and CYP3A4. There was no interaction between the isoenzyme CYP1A2 and the molecules according to the results. Out of five, four molecules inhibited three enzymes. The molecule 2059819 interacted with two enzymes only.

According to the ADME evaluation, none of the studied molecules can permeate the brain by overcoming the barrier. Except 2059819, all molecules possessed low GI absorption behavior. The enhanced GI

absorption of 2059819 may be due to the low LogP and molar refractivity. The combined effect of the cyclopropane ring and the cyanide group present in the molecule was effective to help the quick absorption in the GI system. When comparing the structures of the cyanide substituted molecules (W045, 2059013, 2059819) it is clear that the distance between the tertiary nitrogen and the CN group is shorter in 2059819 than the other molecules.

The permeability glycoprotein (P-glycoprotein or P-gp) is found in many organs of animals, bacteria, and fungi. They are also called multidrug-resistant proteins and are responsible for the efflux of a large range of toxins with the assistance of ATP. Similar to Cytochrome P450 enzymes, P-gp plays an important role in the removal of toxins and drug-drug interactions. They act as a membrane efflux pump and help to pass the substrate inside and outside the cells. The efficacy of some drugs may be reduced if they are thrown out by the P-gp to the lumen (P-gp substrates). The substrates of P-gp may act as inhibitors or inducers. Inhibition of P-glycoprotein by the drugs will improve bioavailability. The pharmacokinetics table revealed that the W045 and 2059020 act as P-gp substrates. The remaining three molecules did not interact with the P-gp appreciably according to the SwissADME study. The inhibition or induction nature of the molecules can't be predicted with the help of SwissADME.

The drug-likeness of the five molecules was evaluated and displayed in Table 4. This property of the molecules are predicted by considering molecular mass, number of hydrogen bond donors, number of hydrogen bond acceptors, topological surface area,

Table 4 — Druglikeness of the ligands predicted by SwissADME

Molecule	Lipinski	Ghose	Veber	Egan	Muegge	Bioavailability Score
W045	Yes	No; 1 violation: MW>480	Yes	Yes	Yes	0.55
2059013	Yes	No; 1 violation: WLOGP>5.6	Yes	Yes	Yes	0.55
2059019	Yes	Yes	Yes	Yes	Yes	0.55
2059020	Yes	No; 1 violation: MW>480	Yes	Yes	Yes	0.55
2059819	Yes	Yes	Yes	Yes	Yes	0.55

Table 5 — Binding affinity of molecules (negative value) on various targets (kcal/mol)

	W045	2059013	2059019	2059020	2059819
6LU7	9.15	8.82	8.83	9.29	8.47
6M3M	9.08	9.81	8.84	9.83	9.32
6VXX(S1/S2)	8.03/8.43	7.47/8.49	7.88/8.85	8.34/8.20	7.37/8.24
6ZCT	8.67	8.59	9.05	9.04	8.86
7K3G	8.31	8.36	8.59	9.34	8.65

molar refractivity, and LogP values. Five scientists (Lipinski, Ghose, Veber, Egan, and Muegge) used various parameters given above and predicted the drug-likeness of molecules. Even though about 50% of the drugs available in the market obey the rules predicted by various scientists, these rules have received considerable attention in drug discovery. All the parameters of five molecules displayed by SwissADME are well suited to the drug-likeness rules such as Lipinski, Veber, Egan, and Muegge. The only violation is noted in the case of Ghose's prediction about drug-likeness. Molecules such as W045, 2059013, 2059020 showed one violation each for the Ghose rule *i.e.*, MW>480, WLOGP>5.6. Thus it is clear that the investigated molecules possess a great extent of drug-likeness.

Molecular Docking Studies

Table 5 represents the docking score of five drug-like molecules on various targets of SARS-CoV-2. High score values of receptor-ligand complexes are marked in bold letters in the table and the details are given in the discussion part. Molecules W045 and 2059020 displayed >9 kcal/mol on the main protease 6LU7. Highest binding affinities (>9.8 kcal/mol) were shown by 2059013 and 2059020 on the nucleocapsid protein having PDB id 6M3M. The receptor-binding domain of the spike protein well interacted with the ligand 2059020 and showed a score of 8.34 kcal/mol on the S1 subunit. 2059019 and 2059020 were the firmly bound molecules on the non-structural protein (NSP10) 6ZCT and showed affinities 9.05 and 9.04 respectively. The only molecule which showed a binding score >9 kcal/mol on the envelope protein 7K3G was 2059020. On comparing the binding scores

of molecules on various receptors, it is evident that the ligand 2059020 possessed the highest docking score on all target proteins of SARS-CoV-2. Details of ligand interactions with the receptor proteins are discussed in the subsequent paragraphs and summarized in Table 6. 3D surface and 2D interaction plots of Receptor-ligand complexes are depicted in Fig. 3.

W045-6LU7 complex

The principal binding pocket of the main protease of a covid-19 virus is located on the outer surface. This ligand interacted with the M^{PRO} of SARS-CoV-2 with five conventional H-bonds in the binding site. The free amino group of w045 made two H-bonds with the amino acid residues His163 and Leu141. The carbonyl group of the ligand acted as the site for two H-bond acceptors for amino acids Ser144 and Gly143. Thr26 residue of protein made a strong hydrogen bond with cyanide group of w045. Two non-conventional hydrogen bonds were established between the carbonyl and nitrile group with Asn142 and Thr25 respectively. One important hydrophobic interaction between w045 and protein was between Met49 and the benzene ring of ligand. Chlorine is attached with His41 and two fluorine atoms bound with Glu166 and Asn142 of the main protease. π -S interaction with the benzene ring and S atom of Met165 residue was also seen in the interaction plot (Fig. 3a). Table 6 provides the number, nature, and distance of interaction between ligand atoms and amino acid residues.

2059020-6LU7 complex

The binding energy of this ligand on the main protease was -9.29 kcal/mol. This can be attributed to

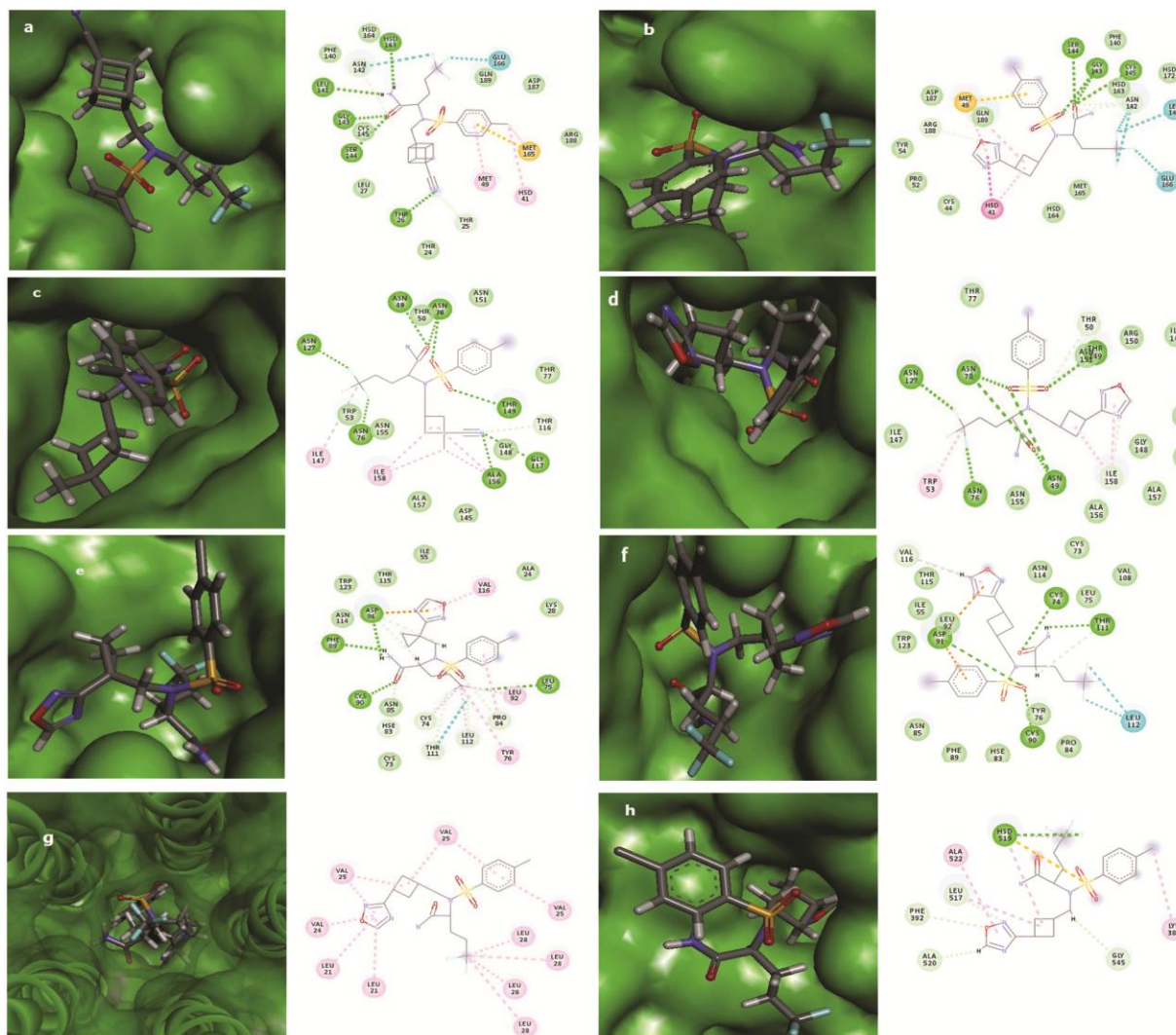


Fig. 3 — 3D Surface and 2D interaction plots of ligand- receptor complexes (a) W045-6LU7 (b) 2059020-6LU7 (c) 2059013-6M3M (d) 2059020-6M3M (e) 2059019-6ZCT (f) 2059020-6ZCT (g) 2059020-7K3G (h) 2059020-6VXX

Table 6 — Details of nature of interaction of drug-like molecules on various receptors

Complex	Interaction	No.	Interacting residues
W045- 6LU7	H-bond	5	His163(2.70 Å), Leu141(2.89Å), Ser144(2.67Å), Gly143(2.17Å), Thr26(2.43Å)
	NC	2	Thr25(2.75Å), Asn142(2.43Å)
	X	3	Cl-His41(4.94Å), F-Glu166(3.57Å), F-Asn142(3.04Å)
	HP	1	Met49(4.95Å)
	π -S	1	Met165(5.87Å)
2059020-6LU7	H-bond	5	Ser144(2)(2.98Å&2.41Å),Cys145(2.96Å), Gly143(2)(2.45Å&(2.63Å)
	NC	3	Asn142(2)(2.52Å&2.74Å), Arg188(2.35Å),
	X	4	F-Leu141(3.19Å), F-Asn142(2)(2.79 Å&2.91Å), F-Glu166(3.31Å),
	HP	1	His141(2)(4.66Å, 4.44Å), Met49(4.0Å)
	π -S	1	Met49(4.89Å)
2059013- 6M3M	H-bond	6	Ala156(2.61Å), Gly117(2.77Å),Thr149(2.19Å), Asn78(2.05Å), Asn78(2.72Å), Asn49(2.02Å)
	NC	1	Thr116(2.59Å),
	X	2	F-Asn76(2.35Å), F-Asn127(2.11Å)
	HP	4	Ile158(5.14Å), Ala156(5.04Å), Ile158(4.67Å), Ala156(3.91Å), Ile147(5.41Å),

(Contd.)

Table 6 — Details of nature of interaction of drug-like molecules on various receptors (*Contd.*)

Complex	Interaction	No.	Interacting residues
2059020- 6M3M	H-bond	5	Asn78(2)(2.56Å& 1.99Å), Asn49(2)(1.98Å& 2.81Å), Thr149(2.19Å),
	NC	2	Thr50(2.55Å), Ile158(2.62Å),
	X	2	F-Asn127(2.72Å),F- Asn76(2.02Å),
	HP	3	Ile158(2)(4.78Å&4.83Å), Trp53(4.06Å),
2059019- 6ZCT	H-bond	4	Phe89(2.53Å), Asp91(2.51Å), Cys90(2.33Å), Leu75(2.64Å)
	NC	6	Asp91(2)(2.86Å&2.76Å),Cys90(2.77Å), His83(2.52Å), Pro84(2.54Å), Leu112(2.36Å), Thr111(2.9Å),
	HP	6	Leu112(5.1Å), Leu92(5.42Å), Cys74(4.05Å), Val116(4.84Å), Tyr76(5.26Å), Pro84(4.95Å)
	X	1	F-Thr111(3.13Å),
	π (elec)	1	Asp91(3.86Å)
2059020- 6ZCT	H-bond	3	Cys74(1.82Å), Asp91(2.5Å), Cys90(2.73Å),
	NC	2	Val116(2.85Å), Thr111(2.74Å),
	HP	1	Val116(5.08Å),
	X	2	F-Leu112(2) (3.35Å& 3.28Å)
	π (elec)	2	Asp91(2) (3.05Å& 4.09Å),
2059020- 7K3g	HP	12	Val25(4.73Å), Val24(4.96Å), Leu21(5.14Å), Leu21(5.47Å), Val25(3.75Å), Val25(2.74Å), Val25(5.49Å), Val25(4.09Å), Leu28(5.06Å), Leu28(4.99Å), Leu28(5.01Å), Leu28(5.14Å)
2059020- 6VXX(S1)	H-bond	1	His519(2.79Å),
	NC	5	Ala520(2.48Å), Phe392(3.07Å), Leu517(2.86Å), His519(2.54Å), Gly524(3.03Å)
	HP	4	Lys386(4.53Å), His519(2)(5.08Å& 4.36Å), Leu517(5.02Å)
	S	1	His519(5.80Å)

NC=Non-conventional hydrogen bonding, HP= Hydrophobic, X=F or Cl, π (elec)= π electrostatic

the increased number of bonds formed between the ligand and protein. Interaction plots revealed the five conventional H-bonds; out of which four originated from the amino acid residues Ser144(2), Cys145, and Gly143 and combined with the C=O of amide linkage. One of the sulphonyl groups also acted as the H-bond acceptor site for Gly143. The length of the five H-bonds varied between 2.41-2.98Å (Table 6). The C=O and S=O group involved in the formation of three non-conventional hydrogen bonds with Asn142 and Arg188. Notable interactions between the fluorine atoms and amino acid residues like Leu141, Asn142, and Glu166 helped the firm binding of the molecule in the binding site of the protease. The oxadiazole ring of the ligand made important hydrophobic bonds with His41 and Met49. The cyclobutane part of the molecule also made one hydrophobic interaction with the amino acid His41. The only π -S interaction in the protein-ligand complex was between the benzene ring and Met49. The 2D and 3D interaction plots of 2059020 with the main protease of covid-19 are shown in Fig. 3b.

2059013-6M3M complex

According to x-ray crystallographic studies, the main binding site of the nucleoprotein is located in the inner core of the folded chain. The ligand 2059013 interacted with the binding pocket of 6M3M protein

with six classical H-bonds. A very good value of the docking score of this ligand (-9.81 kcal/mol) revealed the strong binding with the nucleoprotein. Various groups such as nitrile, S=O, and C=O present in the molecule acted as powerful H-bond accepting sites for Ala156, Gly117, Thr149, Asn78, and Asn49. In addition to this, two F atoms in the CF₃ group acted as H-bond acceptors from Asn76 and Asn127 as seen in the 2D interaction plot. Asparagine residues of the protein took a major role in the binding of 2059013 with the nucleoprotein. Ile158 and Ala156 residues present in the binding cavity of the protein made hydrophobic bonds with both the cyclobutane ring of the ligand and the substituted methyl group. Thr116 residue weakly interacted with the terminal cyanide group of the molecule (Fig. 3c). The nature and details of interactions are listed in Table 6.

2059020-6M3M complex

The molecule 2059020 displayed a good binding score of -9.83 kcal/mol in the computational analysis. The nucleoprotein made strong hydrogen bonds with the ligand's C=O and S=O groups. Amino acid residues Asn78 and Asn49 contributed two H-bonds each to the ligand molecule. Thr149 also donated one hydrogen bond to one of the sulphonyl groups of the ligand. In addition to the conventional H-bonds, two fluorine atoms of the molecule interacted with the

hydrogen atoms of Asn127 and Asn76. These strong hydrogen bonds having distances ranging between 1.98-2.81Å made the receptor-ligand complex very stable (Table 6). A carbon-hydrogen bond was formed between the amino acid residue Thr50 and S=O of the ligand. The interaction plot showed that Ile158 made bonds with both the imidazole ring and cyclobutane ring of the molecule. The 2D interaction plot and the binding pocket of nucleoprotein trapped with 2059020 ligand are given in Fig. 3d.

2059019-6ZCT complex

The inner core of the binding pocket of 6ZCT is more hydrophobic than the edges. The molecule was oriented in a fashion to attach its hydrophobic part towards the inner layer of the receptor. The ligand interacted with almost all amino acid residues in the binding pocket. Four H-bonds and several other interactions made the ligand-receptor complex a stable one with a binding score of -9.05 kcal/mol. The NH₂ group of the amide linkage of ligand donated two hydrogen bonds to Phe89 and Asp91 residues while Cys90 and Leu75 residues of the receptor donated hydrogen bonds to the ligand. Five non-conventional hydrogen bonds were formed between the ligand and the non-structural protein which include the interaction between the C=O and S=O groups with Cys90, his83, and Pro84. The CF₃ terminal made two C...H bonds with Leu112 and Thr111. The free carboxylic group of Asp91 interacted with C-H hydrogen of ligand through its two oxygen atoms. The carboxylate group also made electrostatic attraction with the oxadiazole ring of the ligand. The interaction plot of the ligand-receptor complex is shown in Fig. 3e.

In addition to hydrogen bonds, strong hydrophobic interactions will also contribute to the net stability of the receptor-ligand complex. The hydrophobic pocket of the NSP10 receptor made six hydrophobic interactions with this molecule. The carbon atom bearing three fluorine atoms acted as the key site for the hydrophobic interactions with Leu112, Leu92, Cys74, and Tyr76 residues. In addition to these interactions, pi-alkyl bonds were found between the oxadiazole ring and Val116; similarly between benzene ring and Pro84 (Table 6).

2059020-6ZCT complex

The drug-like molecule 2059020 firmly attached to the pocket of 6ZCT and showed binding energy of -9.04 kcal/mol. The molecule interacted with the non-

structural protein NSP10 of coronavirus by making three hydrogen bonds (Fig. 3f). The C=O group of the amide linkage of the molecule acted as a strong H-bond accepting site from the S-H group of Cys74 with a bond length of 1.82Å. In addition to this, the S=O group of the ligand acted as the acceptor for two hydrogen bonds from Asp91 and Cys90. The oxadiazole ring and C-H group of the ligand made non-conventional hydrogen bonds with Val116 and Thr111 respectively. Two electrostatic interactions were noticed between the carboxylate group of Asp91 and benzene and oxadiazole moiety of the molecule. The oxadiazole ring made one more interaction with the residue Val116 which was pi-alkyl in nature. Fluorine atoms present in the molecule interacted with Leu112 residue.

2059020-7K3G complex

The inner core of envelope protein was mainly hydrophobic. The ligand molecule 2059020 interacted with the binding pocket of the protein with 12 strong hydrophobic bonds; no hydrogen bond was formed between the ligand and the receptor (Table 6). Out of the 12 interactions, 6 were contributed by valine residues, and the remaining 6 were contributed by leucine residues present in different protein chains. The oxadiazole made 4 pi-alkyl bonds with Val25, Val24, Leu21 of one protein segment and Leu21 of another protein segment. The cyclobutane ring of the ligand interacted with Val25 of two different protein chains using alkyl linkages. Val25 residues of two adjacent protein segments interacted with the benzene ring *via* hydrophobic pi alkyl bonds. Four Leu28 amino acid residues of four protein chains made hydrophobic alkyl interaction with the carbon atom of the CF₃ group. The receptor-ligand interaction plot and the most suitable pose of the ligand in the binding pocket of the protein are shown in Fig. 3g.

2059020-6VXX(S1) complex

According to docking investigation, the binding energy of ligand 2059020 with the receptor-binding domain of S1 subunit of chain A of spike glycoprotein was -8.34 kcal/mol. The imidazole ring of histidine residue (His519) of the binding pocket of the S1 lobe played a significant role in the interaction of the ligand with the receptor. The molecule made a strong hydrogen bond with the imidazole ring of His519. Five non-conventional hydrogen bonds were established between the molecule and the binding site. The oxadiazole ring of the molecule interacted with

the amino acid residues such as Ala520, Phe392, and Leu517. The fluorine atom and the aliphatic hydrogen atom interacted with the residues His519 and Gly545 respectively. The four-sided ring system of the molecule made two significant hydrophobic bonds with His519 and Leu517. The halogen atoms such as chlorine and fluorine of the molecule made hydrophobic interaction with Lys386 and His519 respectively. The imidazole ring of His519 formed a bond with the sulfur atom of the molecule. The interactions between the ligand and the receptor can be best viewed from Fig. 3h and the distance between the bonding atoms can be seen from Table 6.

Conclusions

Physical properties and drug-likeness of five substituted sulphonamide molecules were determined using the web server Swiss ADME. All the molecules showed good physical characteristics appropriate for a drug molecule. According to the computational analysis, five molecules obeyed Lipinski, Veber, Egan, and Muegge rules. The potency of five drug-like molecules to bind on the target proteins of SARS-CoV-2 was evaluated using molecular docking studies. The majority of ligands showed >9 kcal/mol of binding energy on various target proteins. Molecules which scored high binding energy with the covid-19 proteins are studied and the nature of the ligand-receptor complexes was discussed in this work. Molecule having ChemBL id 2059020 showed great binding capacity on the structural and non-structural target proteins of SARS-CoV-2. *In vitro* studies and clinical trials have to be performed to validate the affinity of the molecules towards the receptors of covid-19 virus.

References

- 1 <https://www.cdc.gov/coronavirus/2019-ncov/symptoms-testing/symptoms.html>.
- 2 https://www.who.int/health-topics/coronavirus#tab=tab_3.
- 3 https://www.worldometers.info/coronavirus/?utm_campaign=homeAdvegas1
- 4 Voysey M, Clemens S A C, Madhi S A, Weckx L Y, Folegatti P M, Aley P K, Angus B, Baillie V L, Barnabas S L, Borat Q E, Bibi S, Briner C, Cicconi P, Collins A M, Colin-Jones R, Cutland C L, Darton T C, Dheda K, Duncan C J A, Emary K R W, Ewer K J, Fairlie L F, Faust S N, Feng S, Ferreira D M, Finn A, Goodman A L, Green C M, Green C A, Heath P T, Catherine H, Hill H, Hirsch I, Hodgson S H C, Alane I, Jackson S, Jenkin D, Joe C C D, Kerridge S, Koen A, Kwatra G, Lazarus R, Lawrie A M, Lelliott A, Libri V, Lillie P J, Mallory R, Mendes A V A, Milan E P, Minassian A M, McGregor A, Morrison H, Mujadidi Y F, Nana A, O'Reilly P J, Padayachee S D, Pittella A, Plested E, Pollock

- K M, Ramasamy M N, Rhead S, Schwarzbald A V, Singh N, Smith A, Song R, Snape M D, Sprinz E, Sutherland R K, Tarrant R, Thomson E C, Török M E, Toshner M, Turner D P J, Vekemans J, Villafana T L, Watson M E E, Williams C J, Douglas A D, Hill A V S, Lambe T, Gilbert S C & Pollard A J, *Lancet*, 397 (2021) 99.
- 5 Sapkal G N, Yadav P D, Ella R, Deshpande G R, Sahay R R, Gupta N, Vadrevu K M, Abraham P, Panda S & Bhargava B, *J Travel Med*, 19 (2021) 1.
- 6 <https://www.bharatbiotech.com/covaxin.html>.
- 7 Singh A K, Phatak S R, Singh N K, Gupta A, Sharma A, Bhattacharjee K, Singh R, *Medrxiv*, 39 (2021) 6492.
- 8 Tulleken C, *BMJ*, 373 (2021) n1174. <https://doi.org/10.1136/bmj.n1174>.
- 9 Jones I & Roy P, *Lancet*, 397 (2021) 642.
- 10 Baraniuk Chris, *BMJ*, 372 (2021) n743. <https://doi.org/10.1136/bmj.n743>.
- 11 Zain Chagla, *Annals Int Med*, 395 (2021) 1569.
- 12 Spinner C D, Gottlieb R L, Criner Gerard J, López J R A, Cattelan A M, Viladomiu A S, Ogbuagu O, Malhotra P, Mullane K M, Castagna A, Chai L Y A, Roestenberg M, Tsang O T Y, Bernasconi E, Turnier P L, Chang S-C, Gupta D S, Hyland RH, Osinusi A O, Cao H, Blair C, Wang H, Gaggar A, Brainard D M, McPhail M J, Bhagani S, Ahn M Y, Sanyal A J, Huhn G & Marty F M, *JAMA*, 324 (2020) 1048.
- 13 Yeming W, Dingyu Z, Guanhua D, Ronghui Du, Jianping Zhao, Yang Jin, Shouzhi Fu, Ling Gao, Zhenshun Cheng, Qiaofa Lu, Yi Hu, Guangwei Luo, Ke Wang, Yang Lu, Huadong Li, Shuzhen Wang, Shunan Ruan, Chengqing Yang, Chunlin Mei, Yi Wang, Dan Ding, Feng Wu, Xin Tang, Xianzhi Ye, Yingchun Ye, Bing Liu, Jie Yang, Wen Yin, Aili Wang, Guohui Fan, Fei Zhou, Zhibo Liu, Xiaoying Gu, Jiuyang Xu, Lianhan Shang MD, Yi Zhang, Lianjun Cao, Tingting Guo, Yan Wan, Hong Qin, Yushen Jiang, Thomas Jaki, Frederick G Hayden, Peter W Horby, Bin Cao, Chen Wang MD, *Lancet*, 395 (2020) 1569.
- 14 Ko W-C, Rolain J-M, Lee N-Y, Chen P-L, Huang C-T, Lee P-I & Hsueh P-R, *Int J Antimicrob Agents*, 55 (2020) 105933.
- 15 Pilkington V, Pepperrell T & Hill A, *J Virus Erad*, 6 (2020) 45.
- 16 Takahashi T, Luzum J A, Nicol M R & Jacobson P A, *NPJ Genom Med*, 5 (2020) 35.
- 17 <https://www.outlookindia.com/newscroll/drugs-for-hiv-being-tried-on-covid19-patient-in-kerala-docs/1772506>.
- 18 Caldas L A, Carneiro F A, Higa L M, Monteiro F L, Silva G P D, Costa L J D, Durigon E L, Tanuri A & Souza W D, *Sci Rep*, 10 (2020). (<https://doi.org/10.1038/s41598-020-73162-5>).
- 19 Du L, He Y, Zhou Y, Liu S, Zheng B-J & Jiang S, *Nat Rev Microbiol*, 7 (2009) 226.
- 20 Schoeman D & Fielding B C, *Virology*, 16 (2019) 69.
- 21 J Alsaadi E A, Jones I M A & Jones I M, *Future Virology*, 14 (2019) 275.
- 22 Cui J, Li F & Shi Z-L, *Nat Rev Microbiol*, 17 (2019) 181.
- 23 Zhang L, Fang X, Liu X, Ou H, Zhang H, Wang J, Li Q, Cheng H, Zhang W, & Luo Z, *Chem Comm*, 56 (2020) 10235.
- 24 Smits V A J, Hernández-Carralero E, Paz-Cabrera M C, Cabrera E, Hernandez-Reyes Y, Hernández-Fernaud J R, Gillespie D A, Salido E, Hernández-Porto M & Freire R, *Biochem Biophys Res Commun*, 543 (2021) 45.

- 25 Das G, Das T, Chowdhury N, Chatterjee D, Bagchi A & Ghosh Z, *Genomics*, 113 (2021) 1129.
- 26 Abdelmageed M I, Abdelmoneim A H, Mustafa M I, Elfadol N M, Murshed N S, Shantier S W & Makhawi A M, *Biomed Res Int*, 2020 (2020) Article ID 2683286. (<https://doi.org/10.1155/2020/2683286>).
- 27 Prajapat M, Sarma P, Shekhar N, Avti P, Sinha S, Kaur H, Kumar S, Bhattacharyya A, Kumar H, Bansal S & Medhi B, *Indian J Pharmacol*, 52 (2020) 56.
- 28 Ibrahim I M, Abdelmalek D H, Elshahat M E & Elfiky A A, *J Infect*, 80 (2020) 554.
- 29 Vankadari N & Wilce J A, *Emerg Microbes Infect*, 9 (2020) 601.
- 30 Lan J, Ge J, Yu J, Shan S, Zhou H, Fan S, Zhang Q, Shi X, Wang Q, Zhang L & Wang X, *Nature*, 581 (2020) 215.
- 31 Muhammad A S, Khan S, Kazmi A, Bashir N & Siddique R, *J Adv Res*, 24 (2020) 91.
- 32 Basu A, Sarkar A & Maulik U, *Sci Rep*, 10 (2020) 17699. (<https://doi.org/10.1038/s41598-020-74715-4>).
- 33 Ong E, Wong M U, Huffman A, He Y, *Front Immunol*, 11 (2020) 1581.
- 34 Clark L K, Green T J & Petit C M, *J Virol*, 95 (2021) 4. (<https://doi.org/10.1128/jvi.02019-20>).
- 35 Roe M K, Junod N A, Young A R, Beachboard D C & Stobart C C, *J Gen Virol*, 102 (2021) 3.
- 36 Lai CC, Shih TP, Ko WC, Hsueh PR. *Int J Antimicrob Agents*, 55 (2020)105924
- 37 Claverie J-M, *Viruses*, 12 (2020) 646. (<https://doi.org/10.3390/v12060646>).
- 38 <https://www.rcsb.org>.
- 39 The PyMOL Molecular Graphics System, Version 1.2r3pre, Schrödinger, LLC
- 40 <https://spirochem.com/catalog/home>.
- 41 <https://www.ebi.ac.uk/chembl/>.
- 42 Grosdidier Aurélien, Zoete Vincent, Michielin Olivier. SwissDock, a protein-small molecule docking web service based on EADock DSS. *Nucleic Acids Res*. 2011;39. doi: 10.1093/nar/gkr366, PMID 21624888.
- 43 BIOVIA, Dassault systèmes, BIOVIA workbook, release (2020); BIOVIA Pipeline Pilot, release 2020. San Diego: Dassault Systèmes; 2020.